Benign synthesis of quinolinecarboxamide ligands, H₂bqbenzo and H₂bqb and their Pd(II) complexes: X-ray crystal structure, electrochemical and antibacterial studies

Soraia Meghdadi, Mehdi Amirnasr, Mahsa Kiani, Farzaneh Fadaei Tirani, Maryam Bagheri & Kurt Job Schenk

View supplementary material

Accepted author version posted online: 28 May 2017.

Submit your article to this journal

Article views: 5

View related articles

View Crossmark data

Benign synthesis of quinolinecarboxamide ligands, H₂bqbenzo and H₂bqb and their Pd(II) complexes: X-ray crystal structure, electrochemical and antibacterial studies

SORAIA MEGHDADI*†, MEHDI AMIRNASR*†, MAHSA KIANI†, FARZANEH FADAEI TIRANI‡, MARYAM BAGHERI† and KURT JOB SCHENK‡

†Department of Chemistry, Isfahan University of Technology, Isfahan 84156-83111, Iran
‡CCC–IPSB, École Polytechnique Fédérale de Lausanne, Le Cubotron, Dorigny, CH-1015 Lausanne, Switzerland

Two carboxamide ligands, H₂bqbenzo {3,4-bis(2-quinolinecarboxamido)benzophenone} and H₂bqb {*N,N′*-bis[(2-quinolinecarboxamide)-1,2-benzene]}, have been prepared using tetrabutylammonium bromide as an environmentally benign reaction medium. Two new Pd(II) complexes, [Pd^{II}(bqbenzo)] (**1**) and [Pd^{II}(bqb)] (**2**), have been synthesized, characterized and their structures determined by single crystal X-ray diffraction. The di-anionic ligands, bqbenzo^{2-} and bqb^{2-}, are coordinated via two N$_{amide}$ atoms and the nitrogens of the two quinoline rings, with Pd−N$_{amide}$ < Pd−N$_{quinoline}$ bond lengths. The geometry around palladium(II) in both complexes is distorted square planar. The electrochemical behaviors of the ligands and their Pd(II) complexes have been investigated by cyclic voltammetry in DMF. An irreversible Pd$^{II/I}$ reduction is observed at –1.06 V for **1** and at –1.177 V for **2**, indicating the influence of the R substituent on the central phenyl ring of carboxamide ligands on the Pd$^{II/I}$ reduction potential. The ligands and palladium complexes were also screened for *in vitro* antibacterial activity. The Pd(II) complexes show strong biological activity against *S.typhi* and *E.coli* as Gram –ve and *B.cereus* and *S.aureus* as Gram +ve bacteria comparable to the antibiotic penicillin. The antibacterial results also reveal that coordination of Pd(II) significantly improves the activity.

*Corresponding authors. amirnasr@cc.iut.ac.ir (M. Amirnasr); smeghdad@cc.iut.ac.ir (S. Meghdadi)

1. Introduction

Palladium(II) complexes have been investigated because of the structural analogy between Pt^{II} and Pd^{II} coordination compounds. This analogy has stimulated the synthesis of many new Pd^{II} complexes and efforts have recently been made to design anticancer drugs based on palladium compounds [1-3]. These compounds have attracted interest due to their applications in catalytic processes [4-8], construction of chemical sensors [9], and for their cytotoxicity and antibacterial activities [10-13]. Numerous Pd(II) complexes with different ligands have been synthesized and their *in vitro* biological activities on various species of bacteria and fungi have been reported [10-14]. The antiviral, antibacterial, antifungal, and *in vitro/in vivo* anticancer activity of many Pd(II) complexes have been reviewed [15, 16].

The amide functional group, a key link in proteins and peptides, is an important ligand construction unit for coordination chemists. The synthesis of transition metal complexes with ligands containing amide functionality has attracted attention due to their potential applications in medicine [17-19], catalysis [20-22], and construction of functional materials and ion selective electrodes [23-25]. The conventional method for synthesis of carboxamide ligands is reaction of amines with the appropriate carboxylic acids in pyridine (a volatile toxic solvent) solution in the presence of an activator such as triphenylphosphite [26-31]. Replacement of hazardous solvents with greener or more eco-friendly materials has become a high priority [32-34]; we have prepared $H_2bqbenzo$ and H_2bqb by a new method recently developed for the synthesis of carboxamide ligands using the environmentally benign ionic liquid, tetrabutylammonium bromide (TBAB), as the reaction medium and eliminating the need for pyridine as a solvent [35]. The simple work-up procedure, the shorter reaction time, and higher efficiency are other advantages of this method. The conventional synthesis of H_2bqb in pyridine has been reported [29].

In continuation of our work on carboxamide compounds [28, 29, 35-42], herein we report the synthesis of H_2bqb and the new ligand $H_2bqbenzo$ (scheme 1) by the benign method and two new complexes, $[Pd^{II}(bqbenzo)]$ (**1**) and $[Pd^{II}(bqb)]$ (**2**). These compounds have been characterized by different spectroscopic methods. The X-ray crystal structures of **1** and **2**, and the spectroscopic and electrochemical properties of these compounds are reported and discussed. The *in vitro* antibacterial activities of both ligands, their palladium complexes, and Pd(OAc)$_2$ against gram –ve and gram +ve bacteria are evaluated. A comparison between the antibacterial

activities of the complexes and that of the free ligands reveals that metal coordination leads to improved antibacterial activity.
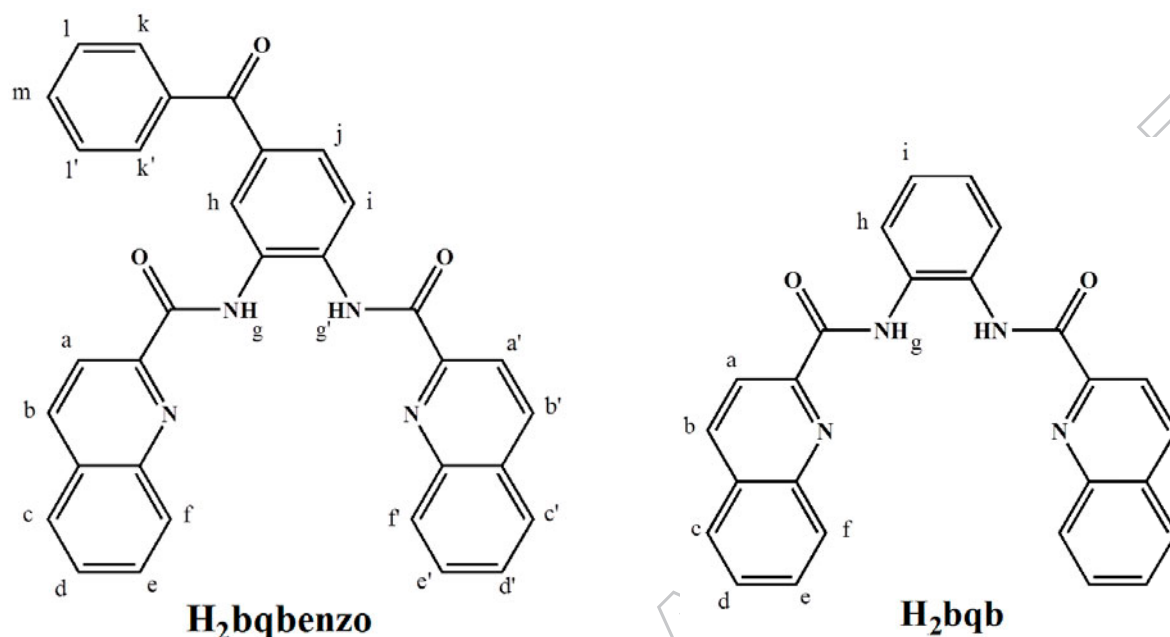
Scheme 1. The chemical formula of H₂bqbenzo and H₂bqb ligands.

2. Experimental

2.1. *Materials and general methods*

All solvents and chemicals were of commercial reagent grade and used as received from Aldrich and Merck. Elemental analyses were performed with a Perkin-Elmer 2400II CHNS-O elemental analyzer. IR spectra were measured with a FT-IR JASCO 680 spectrometer using KBr pellets. UV–visible spectra were recorded on a JASCO V-570 spectrophotometer. ^{1}H NMR spectra were obtained on BRUKER AVANCE III (400 and 500 MHz) spectrometers. Proton chemical shifts are reported in ppm relative to an internal standard of Me$_4$Si (scheme 1). Cyclic voltammograms were recorded by a SAMA 500 Research Analyzer using a three electrode system, a glassy carbon working electrode (Metrohm 6.1204.110 with 2.0 ± 0.1 mm diameter), a platinum disk auxiliary electrode and Ag wire as reference electrode. The glassy carbon-working electrode was manually cleaned with 1 µm alumina polish prior to each scan. CV measurements were performed in DMF with tetrabutylammonium hexafluorophosphate (TBAH) as supporting electrolyte. The solutions were deoxygenated by purging with Ar for 5 min. All electrochemical

3

potentials were calibrated versus the internal $Fc^{+/0}$ (E^0 = 0.45 V vs. SCE) couple under the same conditions [43].

2.2. *Synthesis*

2.2.1. Synthesis of H$_2$bqbenzo. A mixture of triphenylphosphite (3.103 g, 10 mmol), tetrabutylammonium bromide (TBAB) (1.612 g, 5 mmol), quinaldic acid (1.731 g, 10 mmol), and 3,4-diaminobenzophenone (1.061 g, 5 mmol) in a 25 mL round bottom flask was placed in an oil bath. The reaction mixture was heated until a homogeneous solution formed. The solution was stirred for 1 h at 120 °C. The viscous solution was treated with 10 mL methanol and the resulting beige precipitate was isolated by filtration and washed with cold methanol [35]. Yield 64%. Anal. Calc. for $C_{33}H_{22}N_4O_3$: C, 75.85; H, 4.24; N, 10.72. Found: C, 75.68; H, 4.26; N, 10.68%. FT-IR (KBr, cm^{-1}): ν_{max}: 3330 (s, N–H), 1696 (s, C=O$_{amidic}$), 1646 (s, C=O$_{benzo}$), 1588 (s, C=C), 1529 (s, C–N). UV–Vis (DMF): λ_{max} (nm) (ε, L mol^{-1} cm^{-1}): 333 (50080), 293 (96100). ^{1}H NMR (CDCl$_3$, 400 MHz): δ (ppm) = 11.07 (s, 1H, H$_g$), 10.58 (s, 1H, H$_{g'}$), 8.50-8.34 (m, 6H, H$_{a,a',h, i,b,b'}$), 8.08 (d, 1H, H$_j$), 8.96 (d, 1H, H$_k$), 7.91-7.50 (m, 12H, H$_{f,f', e,e',c,c',d,d',k',m,1,1'}$).

2.2.2. Synthesis of H$_2$bqb. This ligand was synthesized by a procedure similar to that of H$_2$bqbenzo except that 1,2-phenylenediamine (0.540 g, 5 mmol) was used instead of 3,4-diaminobenzophenone. Yield 95%. Anal. Calc. for $C_{26}H_{18}N_4O_2$: C, 74.63; H, 4.34; N, 13.39. Found: C, 74.45; H, 4.34; N, 13.37%. FT-IR (KBr, cm^{-1}): ν_{max}: 3320 (s, N–H), 1690 (s, C=O), 1590 (s, C=C), 1530 (s, C–N). UV–Vis (DMF): λ_{max} (nm) (ε, L mol^{-1} cm^{-1}): 315 (15570). ^{1}H NMR (CDCl$_3$, 400 MHz): δ (ppm) = 10.61 (s, 2H, H$_g$), 8.45 (d, 2H, H$_a$), 8.37 (d, 2H, H$_b$), 8.03 (d, 2H, H$_h$), 7.89 (dd, 2H, H$_f$), 7.85 (dd, 2H, H$_c$), 7.60 (m, 4H, H$_{d,e}$), 7.37 (t, 2H, H$_i$) [28].

2.2.3. Synthesis of [Pd^{II}(bqbenzo)] (1). To a solution of Pd(OAc)$_2$ (22.5 mg, 0.1 mmol) in chloroform (160 mL) was slowly added a solution of H$_2$bqbenzo (52 mg, 0.1 mmol) in chloroform (160 mL). To the resulting red orange solution DMSO (16 mL) was added and stirred for 4 h. The reaction mixture was filtered, and dichloromethane (32 mL) was added to the filtrate and placed in the refrigerator. Slow evaporation of this solution afforded dark red crystals of **1a** suitable for X-ray crystallography after 17 days. The crystals were filtered off and dried in vacuum. Yield 95%. Anal. Calc. for $C_{33}H_{20}N_4O_3Pd$: C, 63.22; H, 3.22; N, 8.94. Found: C, 63.09;

4

H, 3.14 N, 8.99%. FT-IR (KBr, cm^{-1}): ν_{max}: 1641 (s, C=O$_{amidic}$), 1594 (s, C=O$_{benzo}$), 1571 (s, C=C), 1555 (s, C–N). UV–Vis (DMF): λ_{max} (nm) (ε, L mol^{-1} cm^{-1}): 440 (3100), 352 (17380), 314 (21040), 298 (19020). ^{1}H NMR (DMSO-d$_6$, 400 MHz): δ (ppm) = 8.91 (t, 2H, H$_{a,a'}$), 8.72 (d, 1H, H$_h$), 8.35 (d, 1H, H$_i$), 8.20 (t, 2H, H$_{b,b'}$), 8.11 (d, 1H, H$_j$), 8.05 (d, 1H, H$_k$), 7.75 (m, 2H, H$_{f,f'}$), 7.68 (m, 4H, H$_{e,,e',c,c'}$), 7.58 (t, 2H, H$_{d,d'}$), 7.43 (d, 1H, H$_{k'}$), 7.37 (dd, 1H, H$_m$), 7.27 (m, 2H, H$_{l, l'}$).

In an alternative procedure, **1** was prepared in chloroform-DMSO (20: 1 v/v), and slow evaporation of the solvent in the refrigerator gave dark red crystals of **1b**, C$_{33}$H$_{20}$N$_4$O$_3$Pd·2(CHCl$_3$), suitable for X-ray crystallography after 13 days.

2.2.4. Synthesis of [Pd^{II}(bqb)] (2). This complex was synthesized by adding a solution of Pd(OAc)$_2$ (22.5 mg, 0.1 mmol) in dichloromethane (120 mL) to a solution of H$_2$bqb (41.6 mg, 0.1 mmol) in chloroform (120 mL). To the resulting red orange solution was added DMSO (12 mL) and stirred for 4 h. The final solution was filtered and dark red crystals suitable for X-ray crystallography were obtained by slow evaporation of the solvent at room temperature after 4 days. The crystals were filtered off and dried in vacuum. Yield 92%. Anal. Calc. for C$_{26}$H$_{16}$N$_4$O$_2$Pd: C, 59.73; H, 3.08; N, 10.72. Found: C, 59.58; H, 3.03 N, 10.51%. FT-IR (KBr, cm^{-1}): ν_{max}: 1619 (s, C=O), 1557 (s, C–N). UV–Vis (DMF): λ_{max} (nm) (ε, L mol^{-1} cm^{-1}): 474 (1890), 312 (22270). ^{1}H NMR (DMSO-d$_6$, 400 MHz,): δ (ppm) = 8.93 (d, 2H, H$_a$), 8.29 (AA′XX′, 2H, H$_h$), 8.20 (d, 2H, H$_f$), 8.13 (d, 2H, H$_b$), 7.69 (t, 2H, H$_e$), 7.45 (d, 4H, H$_c$), 7.23 (t, 2H, H$_d$), 6.94 (AA′XX′, 2H, H$_i$).

2.3. *X-ray crystallography*

Dark red crystals of [Pd^{II}(bqbenzo)] (**1a**) suitable for X-ray crystallography were obtained by slow evaporation of solution of **1** in chloroform-dichloromethane-DMSO (20:2:1 v/v) in the refrigerator. Bragg-intensities of **1a** were collected at the Swiss-Norwegian Beamline at the ESRF, Grenoble, France. A wavelength of 0.69633 Å was selected using a Si(111) double crystal monochromator. A combination of curved mirrors and monochromators produced a focused beam at the crystal position. The crystal was maintained at 100 K using an N$_2$ Cryostream. The data were collected by means of a Pilatus 2M pixel detector from Dectris Ltd. Cell refinement, data reduction, and absorption correction were carried out with the program Crysalis (Version

1.171.35.21) from Agilent Technologies [44]. The structure was solved with direct methods using SIR-2011 [45], and structure refinement on F^2 was performed with SHELXL-2014/7 [46]. All non-hydrogen atoms were refined anisotropically.

Dark red crystals of [Pd^{II}(bqbenzo)] (**1b**) and [Pd^{II}(bqb)] (**2**) suitable for X-ray crystallography were obtained by slow evaporation of solution of **1** in chloroform-DMSO (20:1 v/v) in the refrigerator, and **2** in chloroform-dichloromethane-DMSO (10:10:1 v/v) at room temperature. X-ray intensities of **1b** and **2** were collected on a Stoe IPDS II diffractometer with graphite-monochromated MoKα radiation ($\lambda = 0.71073$ Å). The crystals of **1b** and **2** were maintained at 133 and 95 K, respectively, using an N$_2$ Cryostream. Cell refinement, data reduction and a numerical absorption correction were performed with programs X-AREA (1.62) [47] and XRED32 (1.31) [48]. The structure of **1b** was solved with direct methods using SIR-2004 [49] and that of **2** using SHELXS-97 [46]. The structures were refined using SHELXL-2014/7 by full-matrix least-squares on F^2 [46]. All non-hydrogen atoms were refined anisotropically. Hydrogens were placed in geometrically idealized positions and restrained to ride on their parent atoms. Crystallographic and refinement data are summarized in table 1 for all compounds.

2.4. *Antibacterial activities*

Antibacterial activities of the ligands and corresponding Pd(II) complexes were tested by the well-known diffusion method using Sabouraud dextrose agar and Müller Hinton agar [50]. The zone of inhibition (MZI) was recorded upon completion of the incubation and the mean diameter for each complex at 400 μg mL^{-1} was recorded. Stock solutions were prepared in DMSO. The MZI produced by the compounds were compared with the standard antibiotic Penicillin of similar concentration. Each test was carried out three times to minimize the error. In order to clarify any effect of DMSO in the biological screening, blank studies were carried out, and no activity was observed against any bacterial strains in pure DMSO.

3. Results and discussion

3.1. *Synthesis and characterization*

Since the recognition of ionic liquids as new reaction media and catalysts, these compounds have been used for replacing hazardous solvents, reducing reaction time, and increasing yields of

6

products compared to conventional methods [32-34]. We have used an efficient and benign procedure for the preparation of the two carboxamide ligands, H$_2$bqbenzo and H$_2$bqb, by eliminating the toxic pyridine and using TBAB as the reaction medium [35]. Significant advantages of using TBAB are substitution of pyridine, reduction of the reaction time, simple work up and getting a considerable increase in yields of products. The optimization of the reaction condition by varying reaction temperature, period of heating, and amount of TBAB were examined to obtain the products in high yield. In the preparation of H$_2$bqb carried out by this method, the ligand was obtained in high yield and the reaction time reduced from 4 to 1 h as compared to the conventional method reported [29].

The two new Pd(II) complexes of bqbenzo^{2-} and bqb^{2-} were prepared by reaction of equimolar quantities of the ligands and palladium acetate. Dark red needle-like crystals of Pd(bqbenzo) (**1**) and Pd(bqb) (**2**) suitable for X-ray structure analysis were obtained by slow evaporation of the solvent over a period of several days in the refrigerator and room temperatures, respectively.

3.2. *Description of structure of [Pd(bqbenzo)] (1) and [Pd(bqb)] (2)*

The molecular structures of complexes **1** (**1a**, **1b**) and **2** with the atom numbering scheme are presented in figures 1, 2, 5, and selected bond angles and distances are listed in table 2; both complexes crystallize in monoclinic space group $C2/c$. Both bqbenzo^{2-} and bqb^{2-} are tetradentate di-anionic ligands and bind to the Pd(II) ions via two quinoline and two carboxamide nitrogens, thereby forming three adjacent five-membered chelate rings.

1 (**1a** and **1b**) has a square-planar structure distorted towards a tetrahedron. The *trans* angles N4–Pd1–N2 and N3–Pd1–N1 are 162.6(3)° and 163.6(4)°, indicating that the coordination geometry around the palladium is a distorted puckered square. The angles between *cis* atoms at palladium vary between 78.7(4)° for N3–Pd1–N4 and 117.0(4)° for N1–Pd1–N4. The dihedral angles between the two N,N-chelate rings of 12.86° (Pd1-N1-C9-C10-N2- and Pd1-N3-C32-C33-N4) and 10.34° (Pd2-N5-C42-C43-N6- and Pd2-N7-C65-C66-N8) in **1a** indicate distortion from planarity. This kind of distortion has been reported in related palladium compounds [51]. The Pd–N$_{amide}$ (1.834(14) and 1.939(9) Å) and Pd–N$_{quinoline}$ (2.081(9) and 2.094(9) Å) bond distances of coordinated bqbenzo^{2-} in this complex are similar to those reported for other Pd(II) complexes with deprotonated amide [20, 22, 40]. The Pd–N$_{amide}$ bonds

7

are shorter than the Pd–N$_{quinoline}$ bond length, in accord with deprotonated amide nitrogen being a very strong σ-donor. The average bond distances for C=O (1.22 Å) and C$_{carboxy}$–N (1.36 Å) agree with those reported for related deprotonated amide complexes [20, 40].

1b is solvated with two chloroform molecules per formula unit, only one of which is independent. At T = 133(2) K this chloroform is almost fully ordered, but it nevertheless turned out that a better model was obtained by considering two split orientations. Their threefold axes are tilted, by ~15°, off the intersection of the three mirror planes (Supporting Information, S.2.4). The chloroform molecules are situated between the layers of **1b** and linked to them via intramolecular interactions. The crystal packing of **1b** is illustrated in figure 3. The major and minor parts were refined anisotropically, yielding site occupancy ratios of 0.55 (7) / 0.45 (2). Complex **1b** without the benzoyl group is equivalent to **2** which displays approximate C_2 symmetry. **1b** lies around the twofold axis at (3/4,y,1/2) and therefore presents strict C_2 symmetry. Since there is only one terminal benzoyl group in **1b**, it is necessarily disordered between two orientations (figure 4). Similar to **1a** the average Pd–N$_{amide}$ bond length (1.952 Å) is shorter than the Pd–N$_{quinoline}$ bond length (2.096 Å).

Complex **2** (figure 5) has a square-planar structure by the *trans* angles N2–Pd1–N1^{ii} of 162.03(6)°, indicating that coordination geometry around palladium is distorted square planar. The angles between *cis* atoms at the metal center vary between 80.10(10)° for N1–Pd1–N2 and 117.04(12)° for N1–Pd1–N1^{ii}. The dihedral angle between the two N,N-chelate rings (Pd-N1-C9-C10-N2 and Pd-N1^i-C9^i-C10^i-N2^i) is 13.75°. The average Pd–N$_{amide}$ bond length (1.951(2) Å) agrees with those reported for other deprotonated Pd–N$_{amide}$ bonds (1.957 Å) [20, 22, 40] and is shorter than the Pd–N$_{quinoline}$ bond length (2.087(2) Å). The average bond distances for C=O (1.24 Å) and C$_{carboxy}$–N (1.34 Å) agree well with those reported for related complexes [20, 39].

3.3. *Spectral studies*

FT–IR spectral data of the free ligands, H$_2$bqbenzo and H$_2$bqb, and their Pd(II) complexes are listed in Section 2. FT–IR spectra of the free ligands exhibit a band at 3330 and 3320 cm^{-1}, respectively, corresponding to the v(NH$_{amidic}$) stretch. The absence of N–H stretching band in spectra of the corresponding Pd(II) complexes confirms that the ligands are coordinated in their deprotonated form [22]. The sharp C=O stretching bands at 1696 and 1646 cm^{-1} for H$_2$bqbenzo

8

and at 1690 cm^{-1} for H$_2$bqb are shifted to lower frequencies and appear at 1641 and 1594 cm^{-1} for **1** and at 1619 cm^{-1} for **2**. This is presumably due to resonance enhancement in the deprotonated amide leading to weakening of the C=O bond [22, 52].

The UV–Vis spectra of H$_2$bqbenzo, H$_2$bqb, [Pd^{II}(bqbenzo)] and [Pd^{II}(bqb)] are recorded in DMF solution and the data are presented in Section 2. The absorption spectra of free ligands consist of intense bands at 333 and 293 nm for H$_2$bqbenzo and at 315 nm for H$_2$bqb, that are attributed to intraligand transitions (n→π* and π→π*). The Pd(II) complexes show relatively intense bands in the 298-474 nm region corresponding to intraligand and charge transfer transitions. The absorption band at 440 nm in **1** and at 474 nm in **2** is assigned to the admixture of ligand field and charge transfer transitions [22].

^{1}H NMR spectral measurement of H$_2$bqbenzo was performed in CDCl$_3$ solution and the corresponding data are given in Section 2. The main features of the ^{1}H NMR spectrum of H$_2$bqbenzo are amidic protons N-H at 11.07 and 10.55 ppm [53]. The aromatic protons of this ligand are at 7.54-8.53 ppm. The ^{1}H NMR spectrum of H$_2$bqb is reported [29].

^{1}H NMR spectral measurement of Pd(II) complexes, [Pd^{II}(bqbenzo)] and [Pd(bqb)], were performed in DMSO-d$_6$ solution and the corresponding data are given in Section 2. There are two main features in ^{1}H NMR spectra of the complexes: i) the absence of the amidic proton signal, confirming that the ligands are coordinated in their deprotonated form. ii) The downfield chemical shifts of the aromatic proton signal [53]. The aromatic protons of these compounds are at 6.945-8.94 ppm. Among the aromatic protons, the two H$_{a,a'}$ protons in **1** and the two H$_a$ protons in **2** are the most deshielded and at 8.91 (as two overlapping doublets) and 8.93 ppm (as a doublet), respectively.

3.4. *Electrochemical studies*

The electrochemical behavior of H$_2$bqbenzo and H$_2$bqb and palladium(II) complexes has been studied by cyclic voltammetry in DMF solution at a scan rate of 100 mV s^{-1}, with 0.1 M TBAH as the supporting electrolyte at a glassy carbon working electrode. As expected and previously reported, the carboxamide ligands are electroactive in organic solvents [39]. The three irreversible reduction waves of quinoline rings are observed at –1.482 V, –1.852 V and –2.049 V in the voltammogram of H$_2$bqbenzo (figure 6), and are expected to be shifted to more positive values for **1**. The irreversible reduction wave of the benzophenone ring is at –0.844 V.

The electrochemistry of [Pd(bqbenzo)] (**1**) in DMF (figure 7) shows an additional irreversible reduction process at –1.06 V attributed to reduction of $Pd^{II/I}$. This value is in agreement with those reported in related Pd(II) complexes [54]. The last three irreversible reduction processes at –1.34, –1.67 and –1.92 V are suggested to be mainly ligand centered due to reduction of quinoline rings and are shifted to more positive potentials in Pd(II) complex relative to the free ligand.

The H_2qbq ligand is also electroactive in organic solvents. As shown in the voltammogram of H_2bqb (figure 8), the two irreversible reduction waves of quinoline rings are at –1.56 and –1.87 V and are expected to shift to more positive values in **2**.

The electrochemistry of **2** in DMF (figure 9) shows an irreversible reduction at –1.177 V attributed to reduction of $Pd^{II/I}$, in agreement with those reported in related Pd(II) complexes [54]. The reduction potential of $Pd^{II/I}$ in **1** is more positive (117 mV) than that of **2**, and the difference is presumably due to the electron-withdrawing substituent (benzoyl) in **1**. The electron-withdrawing effect of the benzoyl group is also evident from the energy of the MLCT transition, at 440 nm for **1** as compared to 474 nm for **2** (*vide supra*). There seems to be a good correlation between the reduction potential of Pd(II) complexes and the MLCT transition energy. This is apparently due to a common electronic effect induced by the electron-withdrawing nature of (C(O)Ph) substituent. The last two irreversible reduction processes observed at –1.387 V and –1.49 V are suggested to be mainly ligand centered due to the reduction of quinoline rings and are shifted to more positive potentials in Pd(II) complex relative to the free ligand.

The redox behaviors of Pd(II) carboxamide complexes are influenced by the R substituent on the central phenyl ring of carboxamide ligands. The cyclic voltammetric studies of [$Pd^{II}(Me_2bqb)$] reveal that Me_2bqb^{2-} favors reversibility of the Pd(II)-Pd(III) oxidation process by stabilizing the Pd(III) species, presumably due to the existence of methyl substituents and strong electron donating ability of Me_2bqb^{2-} carboxamide ligand [40]. However, the tendency of [Pd(bqbenzo)] and [Pd(bqb)] to undergo Pd(II)-Pd(I) reduction is in accord with the more electron-withdrawing character of bqb^{2-} and $bqbenzo^{2-}$ ligands as compared to Me_2bqb^{2-}.

3.5. *Antibacterial activity*

The ligands, corresponding Pd(II) complexes and $Pd(OAc)_2$ were tested for antibacterial activities against *Bacillus cereus* and *Staphylococcus aureus* as Gram +ve and *Salmonella typhi*,

Klebsiella pneumoniae and *Escherichia coli* as Gram –ve bacteria. The screening results (MZI) are summarized in table 3. H$_2$bqbenzo and H$_2$bqb show lower antibacterial activity relative to penicillin for *Escherichia coli*, *Staphylococcus aureus* and *Bacillus cereus* (MZI = 6, 16 and 15 mm for H$_2$bqbenzo, MZI = 11, 10 and 12 mm for H$_2$bqb, and MZI = 23, 44, 40 for penicillin, table 3). However the [Pd(bqbenzo)] complex exhibits strong biological activity against *E.coli* as Gram –ve and *B.cereus* and *S.aureus* as Gram +ve species (MZI = 22, 35 and 26, respectively), comparable to the antibiotic penicillin (MZI = 23, 44 and 40, respectively). This complex is not that effective against *Salmonella* and *Klebsiella* and has a small MZI (MZI = 12 and 9, respectively) compared to penicillin (MZI = 38, 16). The [Pd(bqb)] complex has a high growth inhibitory effect on *S.typhi* and *E.coli* as Gram –ve (MZI = 25 and 30) and *B.cereus* and *S.aureus* as Gram +ve species (MZI = 29 and 28 respectively), comparable to that of penicillin (MZI = 38, 23, and 44, 40, respectively). Moreover, the antibacterial effect of these complexes on *S.typhi*, *Klebsiella*, *E.coli*, *B.cereus* and *S.aureus* is more than that reported for Pd(II) complexes with several heterocyclic ligands, for example: the MZI of [Pd(L^{1}H$_2$)Cl$_2$], [Pd (L^2)$_2$] and [Pd (L^3)$_2$] for *E.coli* are 10, 8, and 13 mm, and for *S. aureus* are 9, 7, and 11 mm, respectively) [55], [Pd(MpipDTC)$_2$] and [Pd(DBzDTC)$_2$] (MZI = 18 and 14, respectively) on *S.typhi* [56], [Pd(Ph$_2$PzTSC)$_2$] (MZI = 0, 0, 14 mm) on *E.coli*, *Klebsiella* and *S. aureus* [57], and [Pd(pyrm)$_2$Cl$_2$] (MZI = 0, 0 and 12 mm) on *E.coli*, *B.cereus* and *S. aureus* respectively [58]. A comparison between the antibacterial activity of the [Pd(bqbenzo)] and [Pd(bqb)] complexes with that of the free ligands revealed that coordination improved the antibacterial activity; Pd(OAc)$_2$ did not exhibit any antibacterial activity (table 3).

The results suggest that the antibacterial activity occurs due to synergy between the metal and the ligand. This finding indicated that the metal ion improved the antibacterial activity compared to that of the free ligands. This behavior can be explained by the Overtone's concept of cell permeability [59] and Tweedy's chelation theory [60].

4. Conclusion

This paper describes the synthesis and characterization of two tetradentate carboxamide ligands and their Pd(II) complexes. The coordination geometry around Pd(II) in these complexes is distorted square planar. Complex **1** with the benzoyl substituent on the central phenyl ring of carboxamide ligand was prepared under two different experimental conditions giving **1a** with no

11

solvent and **1b** as the chloroform solvate **1b**·2CHCl$_3$. In **1b** the benzoyl group is disordered between two orientations. An irreversible Pd(II)–Pd(I) reduction process is observed in the CV of the palladium complexes. A good correlation exists between the reduction potential of Pd(II) complexes and the MLCT transition energy, presumably due to a common electronic effect induced by the electron-withdrawing nature of (C(O)Ph) substituent on the bqbenzo^{2-} carboxamide ligand. The ligands and the corresponding palladium complexes were also screened for their *in vitro* antibacterial activity. A comparison between the antibacterial activity of the complexes and that of the free ligands revealed that coordination of Pd(II) improved the activity. The Pd(II) complexes have strong biological activity against *E.coli* as Gram –ve and *B.cereus* and *S.aureus* as Gram +ve bacteria comparable to that of penicillin.

Appendix A. Supplementary data

Crystallographic data for the structural analyses have been deposited with the Cambridge Crystallographic Data Centre, CCDC No. 1451919 for **1a**, No. 1451918 for **1b**, and No. 1451920 for **2**. These data can be obtained free of charge from the Cambridge Crystallographic Data Centre *via* www.ccdc.cam.ac.uk/data_request/cif.

Acknowledgements

References

[1]   A.C. Moro, A.E. Mauro, A.V.G. Netto, S.R. Ananias, M.B. Quilles, I.Z. Carlos, F.R. Pavan, C.Q.F. Leite, M. Horner. *Eur. J. Med. Chem.*, **44**, 4611 (2009).

[2]   J. Quirante, D. Ruiz, A. Gonzalez, C. López, M. Cascante, R. Cortés, R. Messeguer, C. Calvis, L. Baldomà, A. Pascual, Y. Guérardel, B. Pradines, M. Font-Bardía, T. Calvet, C. Biot. *J. Inorg. Biochem.*, **105**, 1720 (2011).

[3]   N.T. Abdel Ghani, A.M. Mansour. *J. Mol. Struct.*, **991**, 108 (2011).

[4]   M. Terasawa, K. Kaneda, T. Imanaka, S. Teranishi. *J. Catal.*, **51**, 406 (1978).

[5]   N. Miyaura, A. Suzuki. *Chem. Rev.*, **95**, 2457 (1995).

[6]   S. Muthumari, N. Mohan, R. Ramesh. *Tetrahedron Lett.*, **56**, 4170 (2015).

[7]   A.F. Littke, G.C. Fu. *Angew. Chem. Int. Ed.*, **41**, 4176 (2002).

[8]   W. Zhang, M. Shi. *Tetrahedron Lett.*, **45**, 8921 (2004).

[9]   S. Antonaroli, B. Crociani, C.D. Natateb, S. Nardis, M. Stefanelli, R. Paolesse. *Sens. Actuators B: Chem.*, **208**, 334 (2015).

[10]   N.T.A. Ghani, A.M. Mansour. *Inorg. Chim. Acta*, **373**, 249 (2011).

[11]   S.J. Sabounchei, P. Shahriary, S. Salehzadeh, Y. Gholiee, D. Nematollahi, A. Chehregani, A. Amani, Z. Afsartala. *Spectrochim. Acta, Part A*, **135**, 1019 (2015).

[12]   C. Biswas, M. Zhu, L. Lu, S. Kaity, M. Das, A. Samanta, J.P. Naskar. *Polyhedron*, **56**, 211 (2013).

[13]   A.M. Plutín, R. Mocelo, A. Alvarez, R. Ramos, E.E. Castellano, M.R. Cominetti, A.E. Graminha, A.G. Ferreira, A.A. Batista. *J. Inorg. Biochem.*, **134**, 76 (2014).

[14]   D.R. Ilić, J.M. Vujić, I.D. Radojević, O.D. Stefanović, L.R. Čomić, D.D. Banković, S.R. Trifunović. *Hem. Ind.*, **66**, 349 (2012).

[15]   A. Garoufis, S.K. Hadjikakou, N. Hadjiliadis. *Coord. Chem. Rev.*, **253**, 1384 (2009).

[16]   M.N. Alam, F. Huq. *Coord. Chem. Rev.*, **316**, 36 (2016).

[17]   J. Martinelli, B. Balali-Mood, R. Panizzo, M.F. Lythgoe, A.J.P. White, P. Ferretti, J.H.G. Steinke, R. Vilar. *Dalton Trans.*, **39**, 10056 (2010).

[18]   N. Kushwaha, R.K. Saini, S.K.S. Kushwaha. *Int. J. Chem. Tech. Res.*, **3**, 203 (2011).

[19]   N.J. Wheate, V. Vora, N.G. Anthony, F.J. McInnes. *J. Incl. Phenom. Macrocycl. Chem.*, **68**, 359 (2010).

[20]   P. Srinivas, P.R. Likhar, H. Maheswaran, B. Sridhar, K. Ravikumar, M.L. Kantam. *Chem. Eur. J.*, **15**, 1578 (2009).

[21]   S. Yadav, S. Kumar, R. Gupta. *Inorg. Chem. Front.*, 2017, DOI: 10.1039/C6QI00389C.

[22]   S. Kumar, R.R. Jha, S. Yadav, R. Gupta. *New J. Chem.*, **39**, 2042 (2015).

[23]   N.J. Hurley, J.J. Hayward, J.M. Rawson, M. Murrie, M. Pilkington. *Inorg. Chem.*, **53**, 8610 (2014).

[24]   H.A. Zamani, M.R. Ganjali, P. Norouzi, S. Meghdadi. *Anal. Lett.*, **41**, 902 (2008).

[25]   H.A. Zamani,. S. Harimi,. M.R. Abedi,. S. Meghdadi. *J. Chem. Pharm. Res.*, **3**, 630 (2011).

[26]   O. Belda, C. Moberg. *Coord. Chem. Rev.*, **249**, 727 (2005).

[27]   A.K. Patra, M.J. Rose, K.A. Murphy, M.M. Olmstead, P.K. Mascharak. *Inorg. Chem.*, **43**, 4487 (2004).

[28]   S. Meghdadi, M. Amirnasr, M.H. Habibi, A. Amiri, V. Ghodsi, A. Rohani, R.W. Harrington, W. Clegg. *Polyhedron*, **27**, 2771 (2008).

[29]   S. Meghdadi, M. Amirnasr, V. Langer, A. Zamanpoor. *Can. J. Chem.*, **84**, 971 (2006).

[30]   J. Zhang, X. Ke, C. Tu, J. Lin, J. Ding, L. Lin, H.-K. Fun, X. You, Z. Guo. *BioMetals*, **16**, 485 (2003).

[31]   D.J. Barnes, R.L. Chapman, R.S. Vagg, E.C. Watton. *J. Chem. Eng. Data*, **23**, 349 (1978).

[32]   R.A. Sheldon. *Green Chem.*, **7**, 267 (2005).

[33]   M.J. Earle, K.R. Seddon. *Pure Appl. Chem.*, **72**, 1391 (2000).

[34]   W. Miao, T.H. Chan. *Acc. Chem. Res.*, **39**, 897 (2006).

[35]   S. Meghdadi, K. Mereiter, A. Amiri, N.S. Mohammadi, F. Zamani, M. Amirnasr. *Polyhedron*, **29**, 2225 (2010).

[36]   S. Meghdadi, M. Amirnasr, S.B.H. Moein Sadat, K. Mereiter, A. Amiri. *Monatsh. Chem.*, **145**, 1583 (2014).

[37]   S. Meghdadi, M. Amirnasr, A. Amiri, Z. Musavizadeh Mobarakeh, Z. Azarkamanzad. *C. R. Chimie*, **17**, 477 (2014).

[38]   S. Meghdadi, K. Mereiter, M. Amirnasr, F. Karimi, A. Amiri. *Polyhedron*, **68**, 60 (2014).

[39]   S. Meghdadi, M. Amirnasr, Z. Azarkamanzad, K. J. Schenk, F. Fadaee, A. Amiri, S. Abbasi. *J. Coord. Chem.*, **66**, 4330 (2013).

[40]   S. Meghdadi, V. Langer, H. Farrokhpour, A. A. Massoud, M. Amirnasr. *J. Iran. Chem. Soc.*, **9**, 85 (2012).

[41]   S. Meghdadi, M. Amirnasr, K. Mereiter, A. Amiri, V. Ghodsi. *Inorg. Chim. Acta*, **363**, 1587 (2010).

[42]   A. Amiri, M. Amirnasr, S. Meghdadi, K. Mereiter, V. Ghodsi, A. Gholami. *Inorg. Chim. Acta*, **362**, 3934 (2009).

[43]   N.G. Connelly, W.E. Geiger. *Chem. Rev.*, **96**, 877 (1996).

[44]   CRYSALIS, Oxford Diffraction Ltd., Abingdon, UK (2006).

[45]   M.C. Burla, R. Caliandro, M. Camalli, B. Carrozzini, G.L. Cascarano, C. Giacovazzo, M. Mallamo, A. Mazzone, G. Polidori, R. Spagna. *J. Appl. Cryst.*, **45**, 351 (2012).

[46]   G.M. Sheldrick. *Acta Cryst*., **A64**, 112 (2008).

[47]   X-AREA; Version 1.62, Stoe & Cie, Darmstadt, Germany (2011).

[48]   X-RED32; Version 1.31, Stoe & Cie GmbH, Darmstadt, Germany (2005).

[49]   M.C. Burla, R. Caliandro, M. Camalli, B. Carrozzini, G.L. Cascarano, L. De Caro, C. Giacovazzo, G. Polidori, R. Spagna. *J. Appl. Crystallogr*., **38**, 381 (2005).

[50]   S. Magaldi, S. Mata-Essayag, C.H. de Capriles, C. Perez, M. Colella, C. Olaizola, Y. Ontiveros. *Int. J. Infect. Dis*., **8**, 39 (2004).

[51]   M. Kubot, D. Covarrubias, C. Py, F.R. Fronczek, R. Isovitch. *J. Coord. Chem*., **66**, 1350 (2013).

[52]   M. Tyagi, S. Chandra. *J. Saudi Chem. Soc*., **18**, 53 (2014).

[53]   C.-Y. Liao, K.-T. Chan, J.-Y. Zeng, C.-H. Hu, C.-Y. Tu, H.M. Lee. *Organometallics*, **26**, 1692 (2007).

[54]   T. Mukherjee, B. Sen, E. Zangrando, G. Hundal, B. Chattopadhyay, P. Chattopadhyay. *Inorg. Chim. Acta*, **406**, 176 (2013).

[55]   M.K. Samota, G. Seth. *Heteroat. Chem*., **21**, 44 (2010).

[56]   F. Shaheen, A. Badshah, M. Gielen, M. Dusek, K. Fejfarova, D. de Vos, B. Mirza. *J. Organomet. Chem*., **692**, 3019 (2007).

[57]   C. Burgos, E. Ana, L. Tamayo, R. Torrellas-Hidalgo. *Revista U.D.C.A Actualidad & Divulgación Científica*, **17**, 477 (2014).

[58]   P.A. Ajibade, O.G. Idemudia. *Bioinorg. Chem. Appl*., ID 549549, 8 pages (2013).

[59]   R. Prabhakaran, S.V. Renukadevi, R. Karvembu, R. Huang, J. Mautz, G. Huttner, R. Subashkumar, K. Natarajan. *Eur. J. Med. Chem*., **43**, 268 (2008).

[60]   B.G. Tweedy. *Phytopathology*, **55**, 910 (1964).
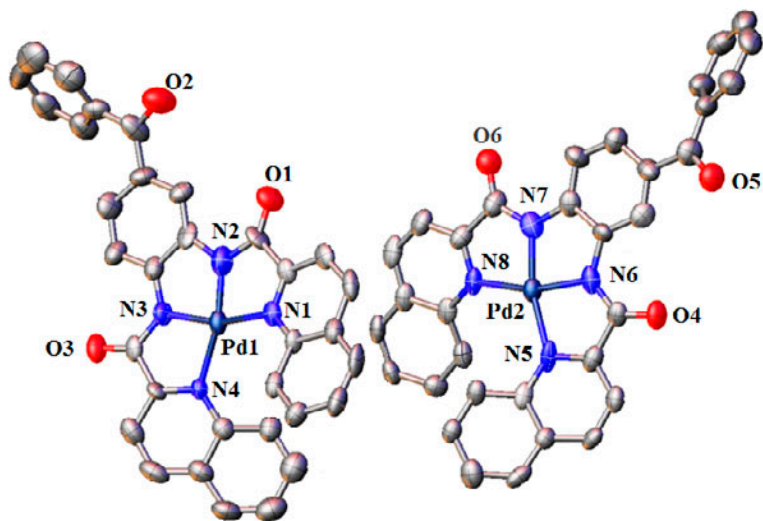
Figure 1. The molecular structure of **1a** with its atom labelling scheme. The displacement ellipsoids are drawn at the 50 % probability level.
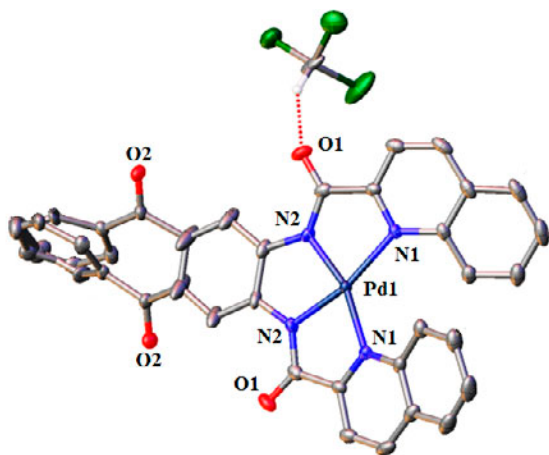
Figure 2. The molecular structure of **1b** with its atom labelling scheme. The displacement ellipsoids are drawn at 50 % probability. Note that only the major of the two orientations of chloroform is shown.
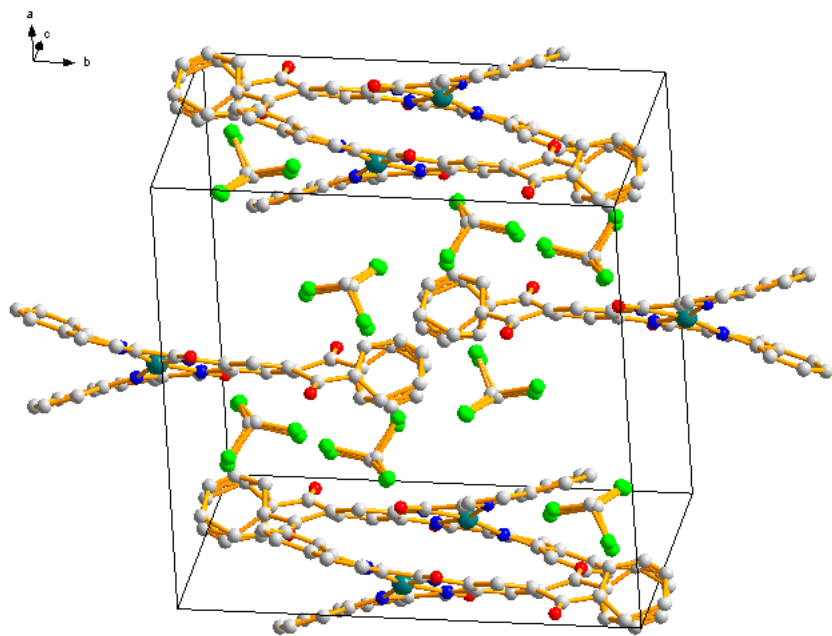
Figure 3. Crystal packing in **1b** as viewed along the crystallographic *a*-axis.
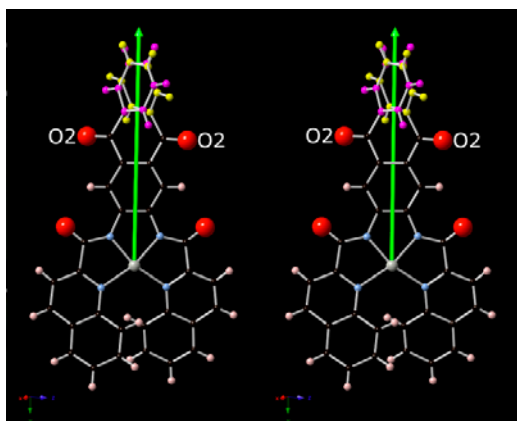
Figure 4. Presentation of the disordered terminal benzoyl group which is necessarily split into two orientations in **1b**.

Figure 5. The molecular structure of **2** with its atom labelling scheme. The displacement ellipsoids are drawn at the 50 % probability level.
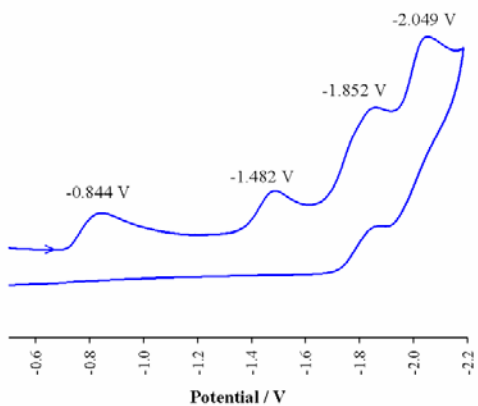
Figure 6. Cyclic voltammogram of H$_2$bqbenzo in DMF at 298 K, c $\approx$ 5×10^{-4}, scan rate = 100 mV s^{-1}.
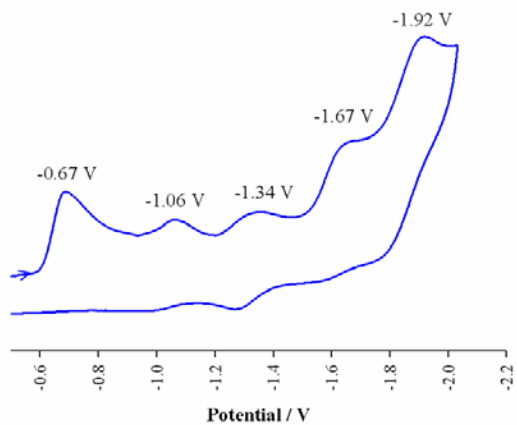
Figure 7. Cyclic voltammogram of [Pd(bqbenzo)] in DMF at 298 K, c $\approx$ 5×10^{-4}, scan rate = 100 mV s^{-1}.
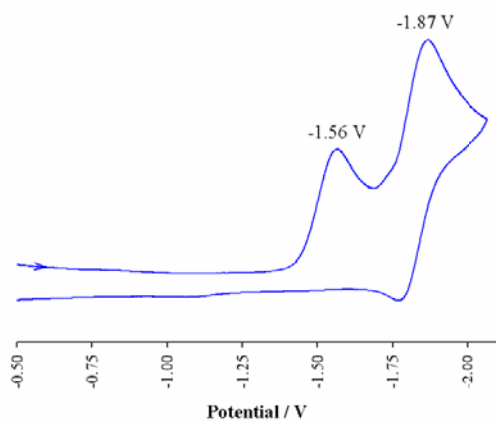
Figure 8. Cyclic voltammogram of H$_2$bqb in DMF at 298 K, c ≈ 5×10^{-4}, scan rate = 100 mV s^{-1}.
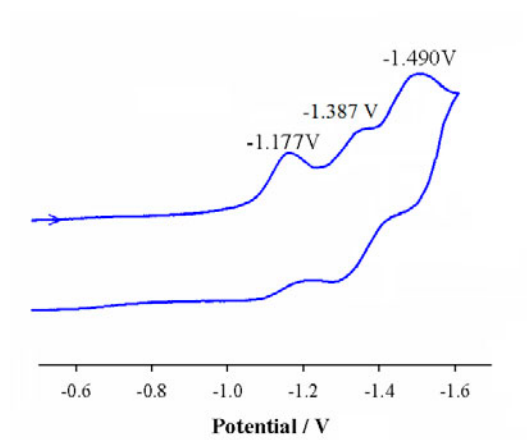
Figure 9. Cyclic voltammogram of [Pd(bqb)] in DMF at 298 K, $c \approx 5 \times 10^{-4}$, scan rate = 100 mV s^{-1}.

Table 1. Crystallographic parameters, data collection and refinement details for **1a**, **1b** and **2**.

Empirical formula	$C_{33}H_{20}N_4O_3Pd$ (**1a**)	$C_{33}H_{19}N_4O_3Pd\cdot 2(CHCl_3)$ (**1b**)	$C_{26}H_{16}N_4O_2Pd$ (**2**)
Formula weight	626.93	864.66	522.83
Radiation, wavelength (Å)	Synchrotron, 0.69633	MoKα, 0.71073	MoKα, 0.71073
Temperature (K)	100(2)	133(2)	95(2)
Crystal system	Monoclinic	Monoclinic	Monoclinic
Space group	$C2/c$	$C2/c$	$C2/c$
a (Å)	24.6595(4)	18.174(9)	17.9005(9)
b (Å)	27.8855(9)	17.854(9)	13.0063(8)
c (Å)	14.4190(3)	10.560(5)	9.0967(5)
β (°)	90.583(2)	90.16(4)	111.145(4)
V (Å^3)	9914.6(4)	3426(3)	1975.3(2)
Z	16	4	4
D_{calc} (Mg/m^3)	1.680	1.676	1.758
μ (mm^{-1})	0.76	1.05	0.98
Crystal size (mm)	$0.125 \times 0.025 \times 0.015$	$0.85 \times 0.04 \times 0.03$	$0.19 \times 0.09 \times 0.07$
$F(000)$	5056	1724	1048
θ range (°)	26.6-1.6	29.4-1.6	29.1-2.4
Index ranges	-31≤h≤31, -25≤k≤25, -17≤l≤17	-24≤h≤24, -24≤k≤24, -13≤l≤14	-24≤h≤23, -17≤k≤17, -12≤l≤12
Absorption correction	Empirical	Integration	Integration
Min. and max. transmission	0.909, 0.989	0.890, 0.970	0.867, 0.958
Reflections collected	22216	20603	9173
R_{int}	0.075	0.091	0.042
Data / restraints / parameters	8128 / 6 / 739	4637 / 32 / 295	2643 / 0 / 150
Goodness-of-fit on F^2	1.09	0.93	1.06
Final R indices [I> 2σ(I)][a]	$R_1 = 0.1171$, $wR_2 = 0.2763$	$R_1 = 0.0404$, $wR_2 = 0.0701$	$R_1 = 0.026$, $wR_2 = 0.0533$
Rindices (all data)	$R_1 = 0.1509$, $wR_2 = 0.3010$	$R_1 = 0.0713$, $wR_2 = 0.0774$	$R_1 = 0.0362$, $wR_2 = 0.0560$
Largest diff. peak / hole (e.Å^{-3})	4.44 / −2.29	0.94 / −1.07	0.63 / −0.90
CCDC number	1451919	1451918	1451920

[a] $R_1 = \sum ||F_o|-|F_c||/ \sum |F_o|$, $wR_2 = \{\sum [w(F_o^2-F_c^2)^2]/ \sum [w(F_o^2)^2]\}^{1/2}$

Table 2. Selected bond lengths (Å) and angles (°) for **1a**, **1b** and **2**.

1a				1b		2	
Bond lengths							
Pd1–N1	2.081(9)	Pd2–N5	2.108(11)	Pd1–N1	2.099(4)	Pd1–N2^{ii}	1.952(2)
Pd1–N2	1.834(14)	Pd2–N6	1.947(9)	Pd1–N2^{i}	1.950(4)	Pd1–N2	1.951(2)
Pd1–N3	1.939(9)	Pd2–N7	1.926(12)	Pd1–N2	1.950(4)	Pd1–N1	2.096(2)
Pd1–N4	2.094(9)	Pd2–N8	2.105(8)	Pd1–N1^{i}	2.099(4)	Pd1–N1^{ii}	2.096(2)
Bond angles							
N2–Pd1–N1	80.3(4)	N6–Pd2–N5	80.0(4)	N2^{i}–Pd1–N2	83.40(2)	N2–Pd1–N2^{ii}	83.40(14)
N2–Pd1–N3	84.5(5)	N7–Pd2–N6	83.3(5)	N2^{i}–Pd1–N1^{i}	80.01(16)	N2^{ii}–Pd1–N1^{ii}	80.50(7)
N3–Pd1–N1	162.7(5)	N7–Pd2–N5	162.4(4)	N2–Pd1–N1^{i}	162.07(14)	N2–Pd1–N1^{ii}	162.14(8)
N2–Pd1–N4	162.5(4)	N6–Pd2–N8	162.0(5)	N2^{i}–Pd1–N1	162.07(14)	N2^{ii}–Pd1–N1	162.14(8)
N1–Pd1–N4	117.0(4)	N8–Pd2–N5	117.1(4)	N1^{i}–Pd1–N1	117.02(2)	N1–Pd1–N1^{ii}	117.04(12)
N3–Pd1–N4	78.7(4)	N7–Pd2–N8	80.2(4)	N2–Pd1–N1	80.10(10)	N2–Pd1–N1	80.10(10)

Symmetry codes: (i) -x,y,3/2-z. (ii) 1-x,y,1/2-z.

Table 3. MZI (mm) for the antimicrobial activity of Pd(OAc)$_2$, H$_2$bqbenzo, H$_2$bqb and their Pd(II) complexes.

Compound	*S. typhi*	*Klebsiella*	*E. coli*	*S. aureus*	*B. cereus*
H$_2$bqbenzo	NI	NI	6 ± 0.22	16 ± 0.36	15 ± 0.25
[Pd(bqbenzo)]	12.5 ± 0.29	9.0 ± 0.41	22 ± 0.43	35.1 ± 0.21	26 ± 0.40
H$_2$bqb	NI	NI	11.2 ± 0.22	10 ± 0.51	12 ± 0.16
[Pd(bqb)]	25 ± 0.40	5 ± 0.16	30 ± 0.25	29 ± 0.73	28 ± 0.16
Pd(OAc)$_2$	NI	NI	NI	NI	NI
Penicillin	38 ± 0.25	16 ± 0.35	23 ± 0.38	44 ± 0.33	40 ± 0.36
DMSO	NI	NI	NI	NI	NI

Data are expressed as the mean ± standard deviation of samples analyzed individually in triplicate.
NI = No inhibition.

Graphical abstract

[Pd(bqbenzo)]

R= H   H₂bqb
R= C(O)Ph   H₂bqbenzo

Pd(OAc)₂

[Pd(bqb)]